| | |
|---|---|
| Title | Partially coherent phase imaging with source shapes estimation |
| Author(s) | Zhong, Jingshan; Tian, Lei; Dauwels, Justin; Waller, Laura |
| Citation | Zhong, J., Tian, L., Dauwels, J., & Waller, L. (2015). Partially coherent phase imaging with source shapes estimation. Proceedings of SPIE - Quantitative Phase Imaging, 9336, 93360O-. |
| Date | 2015 |
| URL | http://hdl.handle.net/10220/26292 |
| Rights | © 2015 Society of Photo-optical Instrumentation Engineers (SPIE). This paper was published in Proceedings of SPIE - Quantitative Phase Imaging and is made available as an electronic reprint (preprint) with permission of Society of Photo-optical Instrumentation Engineers (SPIE). The published version is available at: [http://dx.doi.org/10.1117/12.2078229]. One print or electronic copy may be made for personal use only. Systematic or multiple reproduction, distribution to multiple locations via electronic or other means, duplication of any material in this paper for a fee or for commercial purposes, or modification of the content of the paper is prohibited and is subject to penalties under law. |

# Partially Coherent Phase Imaging with Source Shapes Estimation

Zhong Jingshan[a,b], Lei Tian[b], Justin Dauwels[a] and Laura Waller[b]

[a]Electrical and Electronic Engineering, Nanyang Technological University, Singapore 639798;
[b]Department of Electrical Engineering and Computer Sciences, University of California, Berkeley, CA 94720, USA

## ABSTRACT

We propose a method to recover quantitative phase from a stack of defocused intensity images illuminated with partially coherent light from a source of arbitrary shape in Köhler geometry. The algorithm uses a sparse Kalman filtering approach which is fast, accurate, and robust to noise. The proposed method is able to recover not only the phase, but also the source shape, which defines the spatial coherence of the illumination. We validate our algorithm experimentally in a commercial microscope with biological samples.

**Keywords:** Phase retrieval, Image reconstruction techniques.

## 1. INTRODUCTION

Many imaging systems, such as bright field microscopy, have partially coherent (Köhler) illumination in the Fourier plane of the sample. The Van Cittert-Zernike theory shows that the coherence can be modeled with a simple 2D function, rather than a 4D function, for a general case.[1] The measured defocused intensity can be modeled as a convolution between the intensity that would have been measured with coherent illumination and a scaled source shape.[2] In other words, the measured defocused intensity images are functions of the complex field at focus (phase and amplitude of the object) and the partially coherent illumination shape. Therefore, by treating this as an inverse problem, one is possible to recover both the complex field at focus and the source shape from the measured image stack.

In our work, we use a Kalman filtering approach,[3] which provides the near-optimal phase solution, even in severe noise. The method can be thought of as a hybrid between iterative methods and TIE, in which it uses a nonlinear forward model (as in iterative methods), but updates the phase estimate according to a linearization at each step (as in TIE). Thus, we get the benefits of using a large range of defocus distances, with good convergence. Because the Kalman filter stores an estimate of the noise covariance for all pixels, it provides pixel-wise adaptive filtering, which significantly improves noise performance. Unfortunately, this means that one must store and manipulate a 4D covariance matrix of size $N^2$ (where $N$ is the total number of pixels), so memory requirements are prohibitive. We recently solved this problem by proving that the covariance matrix should be sparse,[4] reducing both memory and computational complexity by many orders of magnitude. The Kalman filter also provides the ability to easily modify the forward model for any complex transfer function. The result is a general method that can achieve nanometer level phase sensitivity, converges reliably and is robust to noise.

However, the previous Kalman filtering phase recovery approach[3,4] only works for the coherent intensity stack. This work focuses on an important extension of our Kalman filter method which enables partially spatially coherent illumination.[2] We restrict our analysis to imaging systems with incoherent sources placed in the Fourier plane of the sample (Köhler geometry). In this configuration, illumination is spatially invariant and coherence is controlled by source shape (via the Van Cittert-Zernike theorem). Smaller sources provide more spatial coherence, usually at the cost of reduced photon flux, lower resolution and unwanted speckle. In some cases, partially coherent light is unavoidable. For example, in lithography applications,[5] current trends towards source-mask optimization (SMO)[6,7] mean that non-traditional source shapes are the norm. Thus, incorporating partial coherence may be not only desirable, but necessary, for phase retrieval.

Contact Laura Waller; E-mail: lwaller@alum.mit.edu

Quantitative Phase Imaging, edited by Gabriel Popescu, YongKeun Park, Proc. of SPIE Vol. 9336, 93360O · © 2015 SPIE · CCC code: 1605-7422/15/$18 · doi: 10.1117/12.2078229

In Section 2, we propose a modification to our Kalman filter method in which coherence effects are modeled as a simple convolution, allowing fast and accurate phase recovery with arbitrary source shape. In Section 3, by adding an extra optimization procedure and some assumptions on the source, we show that it is possible to also recover the source size (coherence) simultaneously, meaning that one need not know the illumination coherence a priori. In Section 4 and 5, we offer experimental results and conclusion.

## 2. PARTIALLY COHERENT PHASE RECOVERY WITH KNOWN SOURCE SHAPE

First, we describe our method for estimating the complex field at focus $A(x, y, z = 0)$ given a known source shape $S(x, y)$. Our dataset consists of multiple intensity images of partially coherent illumination, $I(x, y, z_n)$, taken at different defocus, where $z_n$ is the intensity measurement position along $z$ axis.

Specifically, the convolution model describes the partially coherent intensity $I(x, y, z)$ at defocus distance $z$ as a 2D convolution between the intensity that would have been measured with coherent illumination $|A(x, y, z)|^2$ and a scaled source distribution $S(x, y)$:[8,9]

$$I(x, y, z) = |A(x, y, z)|^2 \otimes S\left(-\frac{f}{z}x, -\frac{f}{z}y\right), \tag{1}$$

where $f$ is the focal length of the condenser lens. Based on this model, we formulate a state-space description and develop a sparse Kalman filtering algorithm for phase recovery.

In order to fit into the framework of our state-space model, we first discretize the continuous model. We rasterize the 2D continuous $x - y$ plane $A(x, y, z_n)$ into a column vector $\mathbf{a}_n$ and denote the Fourier transform of $A(x, y, z_n)$ with $\mathbf{b}_n$. Propagation in Fourier domain is written as:

$$\mathbf{b}_{n-1} = \mathbf{K}\mathbf{a}_{n-1}, \tag{2}$$

$$\mathbf{b}_n = \mathbf{H}_n\mathbf{b}_{n-1}, \tag{3}$$

where $\mathbf{K}$ is the discrete Fourier transform (DFT) matrix, and $\mathbf{H}_n$ is a diagonal matrix describing wave propagation by a distance $z_n - z_{n-1}$.

Assuming that intensity measurements incur Gaussian noise,[4] Eq. (1) is discretized as:

$$\mathbf{I}_n = \mathbf{C}_n|\mathbf{a}_n|^2 + \mathbf{v}, \tag{4}$$

where the vector $\mathbf{I}_n$ is the discretized form of $I(x, y, z_n)$, $|\mathbf{a}_n|^2$ is for discretizing $|A(x, y, z_n)|^2$, $\mathbf{C}_n$ is a circulant matrix describing the convolution by $S(-\frac{f}{z_n}x, -\frac{f}{z_n}y)$, and $\mathbf{v}$ is Gaussian vector noise in the measurement with zero mean and covariance $\mathbf{R}_n = \mathrm{diag}(\mathbf{C}_n|\mathbf{a}_n|^2)$. Note that each entry in the vector $|\mathbf{a}_n|^2$ is the square of the absolute value of the corresponding entry in $\mathbf{a}_n$. From the eigenvalue decomposition property of circulant matrices, $\mathbf{C}_n = \mathbf{K}^H\mathbf{S}_n\mathbf{K}$. Here $\mathbf{S}_n$ is a diagonal matrix with its diagonal entries equal to the Fourier transform of the scaled source $S(-\frac{f}{z_n}x, -\frac{f}{z_n}y)$.

We now derive a complex extended Kalman filter, by linearizing the nonlinear observation model:[10]

$$\mathbf{I}_n = \mathbf{C}_n|\hat{\mathbf{a}}_n|^2 + \mathbf{C}_n\mathrm{diag}(\hat{\mathbf{a}}_n^*)(\mathbf{a}_n - \hat{\mathbf{a}}_n) + \mathbf{C}_n\mathrm{diag}(\hat{\mathbf{a}}_n)(\mathbf{a}_n^* - \hat{\mathbf{a}}_n^*) + \mathbf{v}, \tag{5}$$

where $\hat{\mathbf{a}}_n$ is the state predicted from the previous $n - 1$ observations, and Eq. (5) is the first order Taylor series expansion of Eq. (4) with respect to $\hat{\mathbf{a}}_n$. Here $\mathbf{a}_n^*$ denotes the complex conjugate of $\mathbf{a}_n$, and $\mathrm{diag}(\mathbf{a}_n^*)$ is a diagonal matrix with its corresponding diagonal entries equal to the elements in the vector $\mathbf{a}_n^*$.

Summarizing, the augmented model is:

$$\text{state: } \begin{bmatrix}\mathbf{b}_n \\ \mathbf{b}_n^*\end{bmatrix} = \begin{bmatrix}\mathbf{H}_n & 0 \\ 0 & \mathbf{H}_n^*\end{bmatrix}\begin{bmatrix}\mathbf{b}_{n-1} \\ \mathbf{b}_{n-1}^*\end{bmatrix} \tag{6}$$

$$\text{observation: } \mathbf{I}_n = \begin{bmatrix}\mathbf{J}_n & \mathbf{J}_n^*\end{bmatrix}\begin{bmatrix}\mathbf{b}_n \\ \mathbf{b}_n^*\end{bmatrix} - \mathbf{C}_n|\hat{\mathbf{a}}_n|^2 + \mathbf{v}, \tag{7}$$

where $\mathbf{v}$ is white Gaussian noise with covariance $\mathbf{R}_n$,

$$\mathbf{R}_n = \mathrm{diag}(\mathbf{C}_n|\hat{\mathbf{a}}_n|^2), \text{ and } \mathbf{J}_n = \mathbf{C}_n\mathrm{diag}(\hat{\mathbf{a}}_n^*)\mathbf{K}^H. \tag{8}$$

Table 1: Sparse Kalman filter method for partially coherent phase recovery.

(1) Initialization of $\mathbf{b}_0$, $\mathbf{Q}_0$ and $\mathbf{P}_0$.

(2) Prediction: $\hat{\mathbf{b}}_n = \mathbf{H}_n\mathbf{b}_{n-1}; \hat{\mathbf{Q}}_n = \mathbf{Q}_{n-1}; \hat{\mathbf{P}}_n = \mathbf{H}_n\mathbf{P}_{n-1}\mathbf{H}_n$

(3) Update:

$$\hat{\mathbf{a}}_n = \mathbf{K}^H\hat{\mathbf{b}}_n \tag{9}$$

$$\mathbf{Q}_n = \hat{\mathbf{Q}}_n - (\hat{\mathbf{Q}}_n + \hat{\mathbf{P}}_n)(\hat{\mathbf{Q}}_n + \hat{\mathbf{P}}_n + (\hat{\mathbf{Q}}_n)^* + (\hat{\mathbf{P}}_n)^* + \mathbf{S}_n^{-2})^{-1}(\hat{\mathbf{Q}}_n + (\hat{\mathbf{P}}_n)^*) \tag{10}$$

$$\mathbf{P}_n = \hat{\mathbf{P}}_n - (\hat{\mathbf{Q}}_n + \hat{\mathbf{P}}_n)(\hat{\mathbf{Q}}_n + \hat{\mathbf{P}}_n + (\hat{\mathbf{Q}}_n)^* + (\hat{\mathbf{P}}_n)^* + \mathbf{S}_n^{-2})^{-1}(\hat{\mathbf{P}}_n + (\hat{\mathbf{Q}}_n)^*) \tag{11}$$

$$\mathbf{b}_n = \hat{\mathbf{b}}_n + (\mathbf{Q}_n + \mathbf{P}_n)\mathbf{K}\mathrm{diag}(\hat{\mathbf{a}}_n)\mathbf{C}_n\mathbf{R}_n^{-1}(\mathbf{I}_n - \mathbf{C}_n|\hat{\mathbf{a}}_n|^2). \tag{12}$$

From the state space Eq. (6) - (7), we then modify to accommodate the sparse version as in our earlier work.[4] The resulting partially coherent phase retrieval algorithm is summarized in Table 1. The matrices $\mathbf{Q}_0$ and $\mathbf{P}_0$ are initialized as diagonal matrices, so $\mathbf{Q}_n$ and $\mathbf{P}_n$ remain as diagonal matrices during the update in Eq. (10)-(12). Because the matrices $\mathbf{H}_n$, $\mathbf{S}_n$, $\mathbf{Q}_n$, and $\mathbf{P}_n$ Eqs. (10)-(12) are diagonal, the computational complexity of matrix multiplication in the algorithm is reduced to be linear in the size $N$ of the image. Comparing to $\mathcal{O}(N^3)$ in the standard extended Kalman filter, the computational complexity of the sparse algorithm is $\mathcal{O}(N \log N)$. Thus, the algorithm is computationally efficient and can run in nearly real-time, even with complicated source shapes.

## 3. UNKNOWN SOURCE SHAPE ESTIMATION IN PARTIALLY COHERENT PHASE RECOVERY

The algorithm described in Table 1 assumes a known source shape, $S(x, y)$. Any errors in measurement or estimation of the source will result in errors in the recovered phase. To remedy this, we extend our method to the case where the source shape is unknown. Because the sample phase information is imprinted on each of the coherent modes (source points), the resulting through-focus intensity stack contains sufficient information for recovering both phase and source shape. One could, for example, use blind deconvolution to recover the coherent intensity stack from the partially coherent stack, then recover phase from the coherent stack. Here, we aim to solve for both simultaneously within a single algorithm.

Consider the simplified case of source size estimation for a known complex field $\mathbf{a}_0$ and source $S(x, y)$ with parameters $\theta$ (for example, $\theta$ is the radius of a circular source). The problem is to estimate $\theta$ from the measured partially coherent intensity $\mathbf{I}_n$. The estimation of $\theta$ can be formulated as a nonlinear optimization problem:

$$\min_{\theta} \sum_{n=1}^{N} (\mathbf{I}_n - \mathbf{C}_n(\theta)|\mathbf{a}_n|^2)^T(\mathbf{I}_n - \mathbf{C}_n(\theta)|\mathbf{a}_n|^2), \tag{13}$$

where $|\mathbf{a}_n|^2$ can be obtained by defocusing $\mathbf{a}_0$. The solution finds an optimal $\theta$ to minimize the squared error between measurements $\mathbf{I}_n$ and the estimation $\mathbf{C}_n(\theta)|\mathbf{a}_n|^2$.

To estimate both the complex field $\mathbf{a}_0$ and $\theta$ simultaneously, we propose an iterative update to $\mathbf{a}_0^{(i)}$ and $\theta^{(i)}$, where $i$ denotes the iteration number. A flow chart for the algorithm is shown in Fig. 1. The estimation of the complex-field and source shape parameters are updated gradually until the iterations stop. This iterative method provides an approximation to the optimal solutions for $\mathbf{a}_0$ and $\theta$ in terms of the least squares error between the measurement $\mathbf{I}_n$ and the estimated intensity $\mathbf{C}_n(\theta)|\mathbf{a}_n|$.

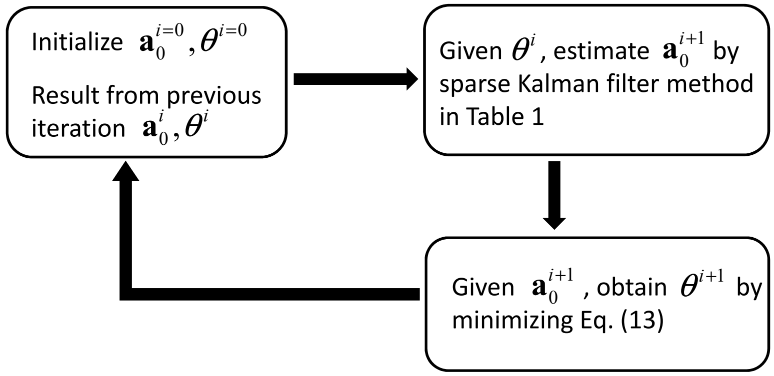


Figure 1: Flow chart of unknown source shape phase recovery.

## 4. EXPERIMENTAL RESULTS

We demonstrate our method experimentally in a Nikon TE300 microscope with broadband illumination centered around wavelength 550 nm. We capture intensity focal stacks of cheek cell samples, using different condenser apertures to vary the source shape (see Fig. 2, top row). The first three shapes were obtained by progressively opening up the condenser aperture to reduce spatial coherence, and the annular ring was obtained by choosing the Ph1 condenser. In order to validate our algorithm, images of the source plane were captured at the side port of the microscope. The measured numerical apertures (NA) of the first three circles are given in top row of Fig. 2, with the two numbers for Ph1 representing the NA of the outer and inner circles. For each shape, the sample was defocused symmetrically about focus at 9 $z$-planes from $1\mu m$ to $16\mu m$, exponentially spaced as in.[11]

The second row of Fig. 2 shows the phase images recovered by our previous method, the coherent Kalman filter.[4] In the case of Size 1, the light source can be approximately viewed as coherent since the source size is small. The coherent Kalman filter thus recovers an accurate phase result. As the size of light source increases, however, the level of coherence reduces and the recovered phase becomes more blurred, degrading the phase result. Next, we test our partially coherent Kalman filter with known (measured) source shapes, showing that it can recover an accurate phase result for each case. Its recovered phase images do not suffer from blurring and contain fine details for all source sizes and shapes, as shown in the third row of Fig. 2. Note that the phase recovered from the larger sources has slightly better resolution than the coherent case, due to the partial coherence of the illumination.

Finally, we show results for our algorithm with both phase and source size recovery. The recovered NA for the source shapes Size 1, Size 2, Size 3, and Ph1 are 0.045, 0.124, 0.203, 0.197 (outer NA of Ph1), and 0.151 (inner NA of Ph1), respectively. The algorithm successfully recovers a source NA similar to the measured values (Fig. 2, top row) and we can see in Fig. 3 that the estimated NA converges after only a few iterations. The phase recovered with the unknown source algorithm also shows good fidelity (Fig. 2, bottom row). In fact, the phase with the unknown source algorithm contains somewhat better details than those with known source shapes, suggesting that the recovered source shapes are more accurate than the measured ones. This suggests that the unknown source algorithm may be used (with the measured source as an initial guess), even when the source shape is known.

In our experiments, we find that the annular aperture provides the best phase result for several reasons. It achieves the improved spatial resolution that comes with using partially coherent illumination, but does not lose contrast through-focus due to blurring, as in the case of the larger circular aperture. Another advantage of using partially coherent illumination is that images do not suffer from speckle noise or out-of-focus artifacts, as the coherent situation. An interesting topic for future work might be to derive the optimal source shape for a given experiment.

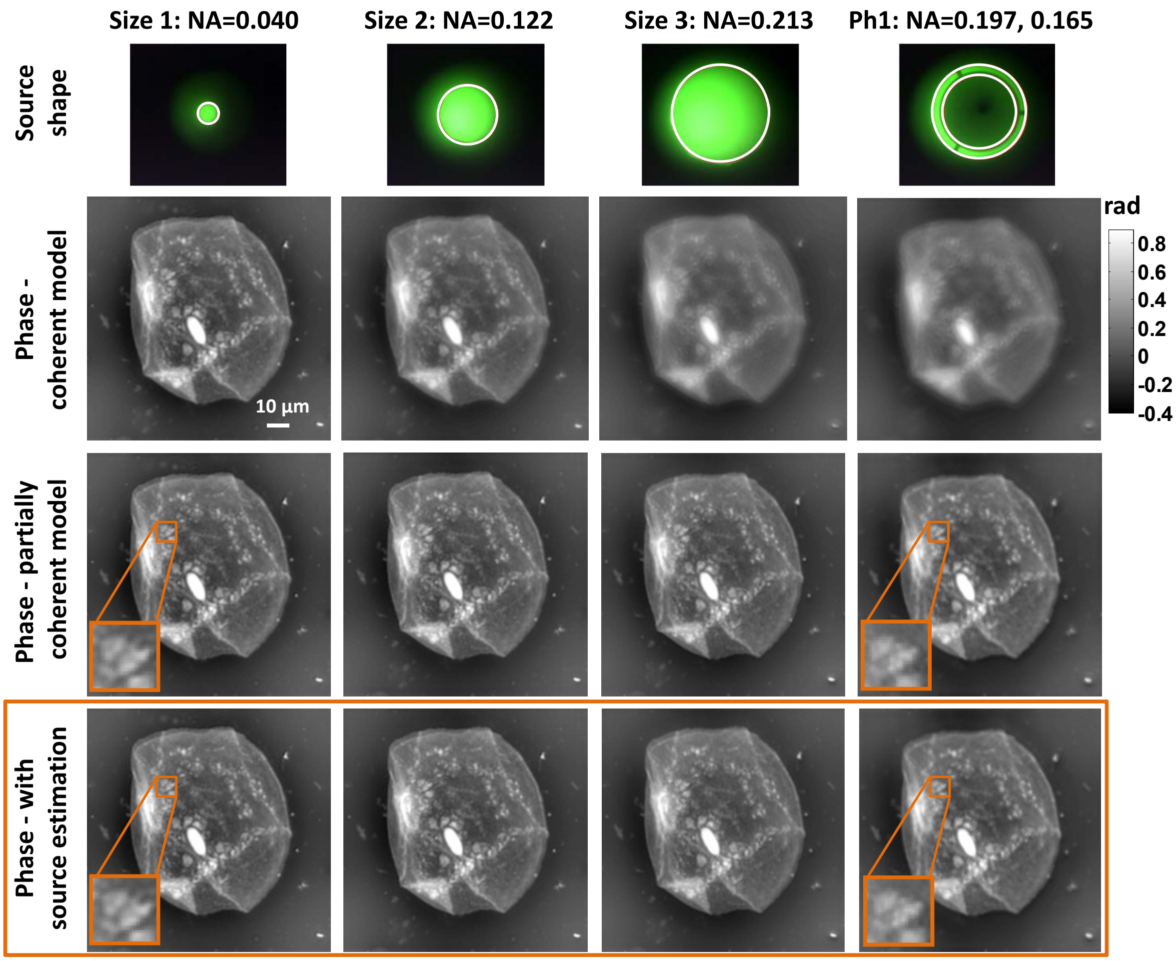


Figure 2: Experimental comparison of phase recovered by the coherent Kalman filter as compared to the partially coherent Kalman filter, both with known and unknown sources. (Top) Measured source shape, with estimated source in white. (Second row) Phase recovered by the coherent Kalman filter is blurred for less coherent sources. (Third row) Phase recovered by the partially coherent Kalman filter (with known source). (Bottom) Phase recovered by the partially coherent Kalman filter with unknown source.

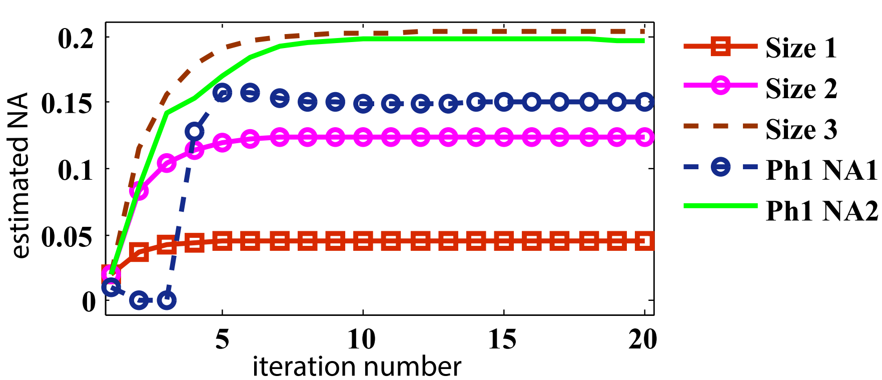


Figure 3: Convergence of source size estimation.

## 5. CONCLUSION

We have demonstrated new Kalman filtering methods to recover phase and illumination coherence from a stack of defocused intensity images. Our algorithm can either incorporate a known source of arbitrary shape, or estimate the source size computationally. This embedded calibration step is particularly helpful for making our algorithm more general and easy to implement. We expect it will find use not only in biological microscopes, but also in X-ray and TEM imaging, where source coherence is difficult to control and may change between experiments.[12] The ability to work with partially coherent illumination, along with the simplicity of phase-from-defocus techniques, eases constraints on experiments, and opening up new application areas.

## Acknowledgments

We thank Dustin Moore for helpful discussions. This work was supported in part by IMPACT+ member companies: Applied Materials, ARM, ASML, Global Foundries, IBM, Intel, KLA-Tencor, Mentor Graphics, Panoramic Tech, Qualcomm, Samsung, SanDisk and Tokyo Electron and the Bakar Fellows Program.

## REFERENCES

1. M. Raymer, M. Beck, and D. McAlister, "Complex wave-field reconstruction using phase-space tomography," *Phys. Rev. Lett.* **72**, pp. 1137–1140, Feb 1994.
2. Z. Jingshan, L. Tian, R. A. Claus, J. Dauwels, and L. Waller, "Partially coherent phase recovery by Kalman filtering," in *Frontiers in Optics*, pp. FW6A–9, Optical Society of America, 2013.
3. L. Waller, M. Tsang, S. Ponda, S. Yang, and G. Barbastathis, "Phase and amplitude imaging from noisy images by Kalman filtering," *Opt. Express* **19**, pp. 2805–2814, Jan 2011.
4. Z. Jingshan, J. Dauwels, M. A. Vázquez, and L. Waller, "Sparse ACEKF for phase reconstruction," *Opt. Express* **21**, pp. 18125–18137, Jul 2013.
5. A. Shanker, L. Tian, M. Sczyrba, B. Connolly, A. Neureuther, and L. Waller, "Transport of intensity phase imaging in the presence of curl effects induced by strongly absorbing photomasks," *Applied Optics* **53**(34), pp. J1–J6, 2014.
6. K. Lai, A. E. Rosenbluth, S. Bagheri, J. Hoffnagle, K. Tian, D. Melville, J. Tirapu-Azpiroz, M. Fakhry, Y. Kim, S. Halle, G. McIntyre, A. Wagner, G. Burr, M. Burkhardt, D. Corliss, E. Gallagher, T. Faure, M. Hibbs, D. Flagello, J. Zimmermann, B. Kneer, F. Rohmund, F. Hartung, C. Hennerkes, M. Maul, R. Kazinczi, A. Engelen, R. Carpaij, R. Groenendijk, J. Hageman, and C. Russ, "Experimental result and simulation analysis for the use of pixelated illumination from source mask optimization for 22nm logic lithography process," in *SPIE Advanced Lithography*, pp. 72740A–72740A, International Society for Optics and Photonics, 2009.
7. R. Socha, X. Shi, and D. LeHoty, "Simultaneous source mask optimization," in *Photomask and Next Generation Lithography Mask Technology XII*, pp. 180–193, International Society for Optics and Photonics, 2005.
8. K. Nugent, "A generalization of Schell's theorem," *Opt. Commun.* **79**(5), pp. 267 – 269, 1990.
9. A. Martin, F.-R. Chen, W.-K. Hsieh, J.-J. Kai, S. Findlay, and L. Allen, "Spatial incoherence in phase retrieval based on focus variation," *Ultramicroscopy* **106**(10), pp. 914 – 924, 2006.
10. D. H. Dini and D. P. Mandic, "Class of widely linear complex Kalman filters," *IEEE Trans. Neural Netw. Learning Syst.* , pp. 775–786, 2012.
11. Z. Jingshan, R. A. Claus, J. Dauwels, L. Tian, and L. Waller, "Transport of intensity phase imaging by intensity spectrum fitting of exponentially spaced defocus planes," *Opt. Express* **22**, pp. 10661–10674, May 2014.
12. J. Clark, X. Huang, R. Harder, and I. Robinson, "High-resolution three-dimensional partially coherent diffraction imaging," *Nature communications* **3**, p. 993, 2012.